Electromagnetic forces in negative-refractive-index metamaterials: A first-principles study

Vassilios Yannopapas* and Pavlos G. Galiatsatos
Department of Materials Science, University of Patras, GR-26504 Patras, Greece
(Received 21 December 2007; published 15 April 2008)

According to the theory of Veselago, when a particle immersed within a metamaterial with negative refractive index is illuminated by plane wave, it experiences a reversed radiation force due to the antiparallel directions of the phase velocity and energy flow. By employing an *ab initio* method, we show that, in the limit of zero losses, the effect of reversed radiation pressure is generally true only for the specular beam. Waves generated by diffraction of the incident light at the surface of the slab of the metamaterial can produce a total force which is parallel to the radiation flow. However, when the actual losses of the materials are taken into account, the phenomenon of reversed radiation force is evident within the whole range of a negative refractive index band.

DOI: 10.1103/PhysRevA.77.043819 PACS number(s): 42.70.Qs, 42.25.Bs, 78.67.Bf, 78.67.Pt

Metamaterials are man-made materials exhibiting response characteristics that are not observed in the individual responses of its constituent materials [1]. The most intriguing class of metamaterials is the one that exhibits simultaneously negative permittivity ϵ and permeability μ, i.e., a negative refractive index (NRI) [2,3]. This latter property opens up the gate to a realm of novel, exotic phenomena such as inverse Snell's law [4], near-field amplification [5], perfect lensing [3], reversed Cherenkov effect [6], and reversed electromagnetic (EM) force (see Fig. 1). This latter phenomenon is one of the least explored phenomena in the optics of NRI metamaterials, apart from a controversial issue on the existence of electromagnetic shear force at the boundary between a NRI and a positive-refractive-index (PRI) medium [7] which has been, however, recently resolved [8]. Moreover, there is complete absence of relevant experimental data. The aim of this paper is to provide a numerical evidence of the reversal of radiation force exerted on a particle immersed in a NRI metamaterial (see Fig. 1) by means of first-principles calculations. We note that a numerical validation of this phenomenon is not known *a priori* since the nature of the EM force acting on a particle embedded in a homogeneous NRI medium whose effective refractive index describes a given metamaterial, is different from the corresponding force when the particle is assumed to be immersed in the *actual* metamaterial. In the first case, and neglecting losses, the resulting EM force on the particle stems from the radiation pressure of an incident plane wave. In the second case, the force stems from the gradient of the EM radiation intensity since the EM field, which reaches a particular point of the actual metamaterial, carries various homogeneous and inhomogeneous components; the latter are generated by the scattering of the incident wave at the surface of the metamaterial. These two different pictures should provide the same effect (reversed EM force) if effective medium description is indeed adequate for the description of the metamaterial.

In order to explore the effect of reversed force from first principles, we have to employ a specific structure exhibiting NRI. As such, we consider a three-dimensional (3D) array of close-packed CuCl nanoparticles of radius $S=28$ nm coated with a Drude-type metal; CuCl exhibits a Z_3 exciton line at 386.93 nm [9]. Around the exciton frequency, the permittivity of the above semiconductor is given by $\epsilon_s(\omega)=\epsilon_\infty+A\gamma_s/(\omega_0-\omega-i\gamma_s)$, where $A=632$, $\epsilon_\infty=5.59$, $\hbar\omega_0=3.363$ eV, and $\hbar\gamma_s=5\times10^{-5}$ eV [9]. As shown recently [10], when collections of such nanospheres are illuminated by externally incident light at the exciton resonance, they exhibit negative effective magnetic permeability μ_{eff} due to the enhancement of the displacement current inside each sphere which, in turn, gives rise to a macroscopic magnetization of the collection of CuCl spheres. By coating the above spheres with a metal, a NRI results in [11]. We coat the CuCl nanoparticles with a metal shell of nanometer thickness, $\ell=0.10S=2.8$ nm (the outer radius is $S=28$ nm). The permittivity of the metal is assumed to be described by the Drude model, i.e., $\epsilon_m=1-\omega_p^2/[\omega(\omega+i\gamma_m)]$. In order to achieve NRI, $\omega_p=1.05\omega_0$. To begin with, we turn off losses in the constituent materials ($\gamma_s=\gamma_m=0$).

The effective permittivity ϵ_{eff} and permeability μ_{eff} of such a structure can be calculated by the extended Maxwell-Garnett (EMG) theory [12], which agrees very well with more rigorous approaches [10,11]. Figure 2(a) shows the effective refractive index n_{eff} for the above described system of metal-coated CuCl nanoparticles. We note that, although

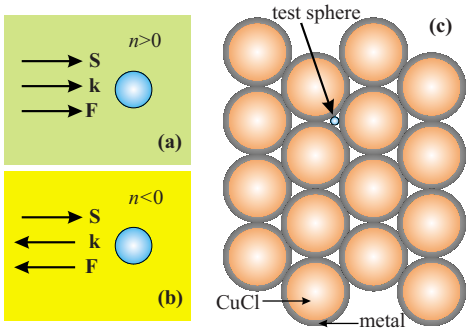

FIG. 1. (Color online) Poynting vector **S**, wave vector **k**, and radiation force **F** exerted on a sphere for a (a) PRI medium and (b) for a NRI medium. In a PRI medium an incident plane wave induces a repulsive force on a sphere while in a NRI one, it induces an attractive force. (c) Calculation setup.

*vyannop@upatras.gr

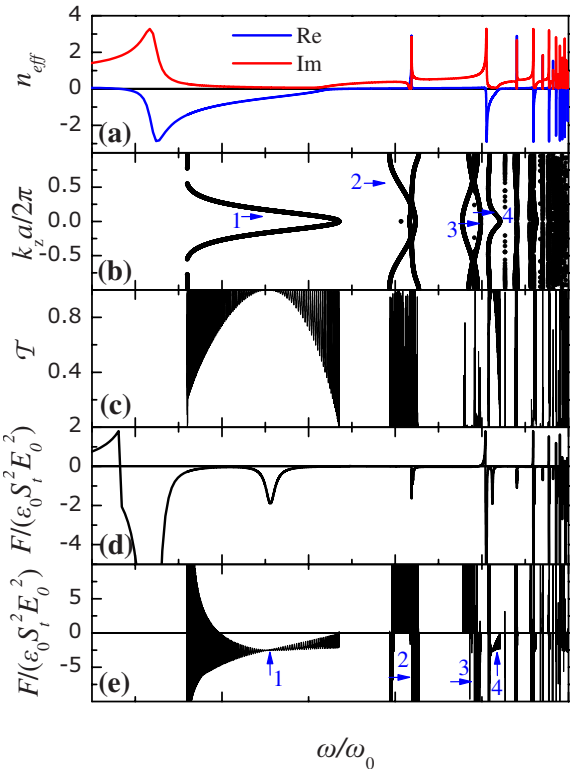

FIG. 2. (Color online) (a) Real and imaginary parts of the effective refractive index n_{eff} of a 3D array of *lossless* close-packed metal-coated CuCl spheres of outer radius $S=28$ nm and coating thickness $\ell=2.8$ nm, as calculated by the EMG method. (b) Frequency band structure normal to the (001) surface of an fcc crystal consisting of the above coated nanospheres, as calculated by the rigorous LMS method. The arrows enumerate the most pronounced NRI frequency bands. (c) Corresponding transmittance curve for light incident normally on a slab consisting of 512 (001) planes of an fcc crystal of the above nanospheres. (d) Spectrum of the EM force exerted on a polystyrene ($\epsilon=2.56$) nanosphere of radius $S=2.9$ nm embedded in a homogeneous medium described by n_{eff} depicted in (a). (e) Spectrum of the EM force exerted on the same sphere as in (d) which is embedded in the middle of the 512-layers-thick slab described in (c) [see also Fig. 1(c)]. The arrows enumerate the NRI frequency regions of (b).

we have neglected losses in the constituent materials for the time being, the EMG theory predicts nonzero values for Im n_{eff} as it is associated with the extinction of the propagating beam due to scattering. Therefore, although n_{eff} can be used to calculate all the optical properties of the medium, it cannot be used directly to evaluate the absorption or the heating rate [12]. We observe that there exist several frequency regions where Re $n_{eff}<0$.

In order to verify the validity of the effective refractive index depicted in Fig. 2(a), we have also employed the layer-multiple scattering (LMS) method [13] for a particular realization of close-packed metal-coated CuCl nanospheres. Namely, we have chosen an fcc lattice, viewed as a succession of (001) planes, whose lattice sites are occupied by the above nanospheres. In Fig. 2(b) we show the frequency band structure normal to the (001) surface [the Bloch wave vector is $\mathbf{k}=(0,0,k_z)$] of an fcc crystal of the above metal-coated nanospheres obtained by the LMS method. We have assumed angular-momentum cutoff $l_{\max}=3$ in the spherical-wave expansion while we have taken into account nine reciprocal lattice vectors in the plane-wave expansion [13]. Since we deal with a close-packed structure, the first-neighbors distance is $a_0=2S$ and the corresponding lattice constant $a=\sqrt{2}a_0=79.2$ nm. We have included only the degenerate frequency bands since only those can couple with normally incident light [13]. It is obvious that there exist several NRI bands (group velocity $\partial\omega/\partial k_z$ antiparallel to the phase velocity ω/k_z), the most prominent of which are enumerated in Fig. 2(b). The first and the fourth NRI bands are in agreement with corresponding NRI regions of Fig. 2(a). The second and third NRI of Fig. 2(b) do not have their counterparts in Fig. 2(a), possibly due to their coexistence with other, positive-refractive-index bands. Figure 2(c) shows the transmittance curve for light incident normally on a slab consisting of 512 (001) planes of the above fcc crystal. It is evident that the transmittance is significant within the NRI frequency bands of Fig. 2(b). The dense structure of oscillations observed in the transmittance curve is due to resonant scattering of light at the slab-air interfaces (Fabry-Pérot oscillations).

Thanks to the rich structure of NRI bands of Fig. 2, the above metamaterial can serve as a testing ground for the numerical study of the phenomenon of the reversed radiation force. We consider a small ($S_t=2.9$ nm) dielectric ($\epsilon=2.56$-polystyrene) test sphere placed in free space, in the middle of a 512-planes-thick metamaterial slab [that of Fig. 2(c)—see Fig. 1(c)]. We wish to calculate the EM force exerted on this test sphere when the slab is illuminated by a normally incident EM wave. Using the LMS formalism [13], the electric field in free space within the slab is written as a sum of plane waves, i.e.,

$$\mathbf{E}(\mathbf{r}) = \sum_{\mathbf{g}} \{\mathbf{E}_{\mathbf{g}}^{+} \exp[i\mathbf{K}_{\mathbf{g}}^{+} \cdot (\mathbf{r}-\mathbf{r}_t)] + \mathbf{E}_{\mathbf{g}}^{-} \exp[i\mathbf{K}_{\mathbf{g}}^{-} \cdot (\mathbf{r}-\mathbf{r}_t)]\}, \tag{1}$$

where $\mathbf{g}$ represents the reciprocal-lattice vectors of the two-dimensional (2D) periodic (square) lattice of a single fcc (001) plane of nanospheres [13] and $\mathbf{K}_{\mathbf{g}}^{\pm}=(\mathbf{k}_{\parallel}+\mathbf{g}, \pm[q^2-(\mathbf{k}_{\parallel}+\mathbf{g})^2]^{1/2})$, with $q=\omega/c$. The sign $+(-)$ corresponds to wave traveling to the positive (negative) direction. $\mathbf{k}_{\parallel}$ is the reduced wave vector which lies within the surface Brillouin zone (SBZ) associated with the reciprocal lattice (for normal incidence $\mathbf{k}_{\parallel}=\mathbf{0}$). $\mathbf{r}_t$ is the position vector of the test sphere. $\mathbf{E}_{\mathbf{g}}^{+}$, $\mathbf{E}_{\mathbf{g}}^{-}$ of Eq. (1) depend linearly on the field amplitude of an incident plane wave through the scattering matrices [13] of the slabs on the left and right side of the test sphere. By solving the Mie-scattering problem for the test sphere with the field of Eq. (1) as the incident field and by integrating analytically the Maxwell stress tensor over the sphere surface, we finally calculate the EM force. For the case where the test sphere is embedded in a homogeneous medium characterized by n_{eff}, the above procedure is much simpler since the wave incident on the sphere is a single plane wave, $\mathbf{E}_0 \exp[i\mathbf{q}\cdot(\mathbf{r}-\mathbf{r}_t)]$, and standard Mie theory applies.

In Fig. 2(d) we show the spectrum of the normalized force

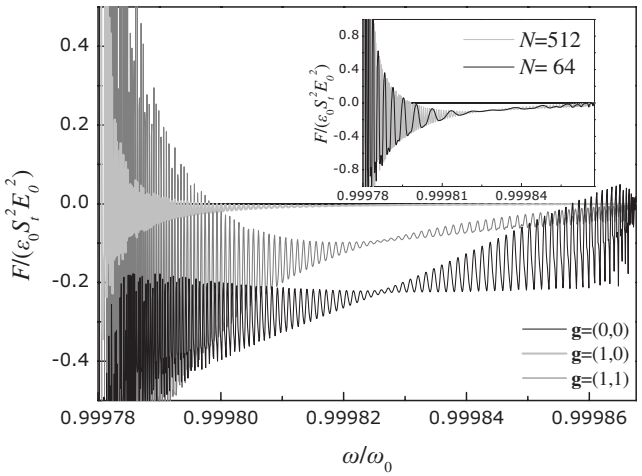

FIG. 3. The force spectrum of Fig. 2(e) within the first NRI band, analyzed into its **g**-vector components (shown in the legend in $2\pi/a_0$ units). The inset shows the force component with $\mathbf{g}=(2\pi/a_0)(1,1)$ for two different slab thicknesses.

$F/(\epsilon_0 S_t^2 E_0^2)$ exerted on the test sphere, which is embedded in a homogeneous medium characterized by the n_{eff} of Fig. 2(a). It is illuminated by a plane wave whose source lies at the test sphere in order to eliminate the artifact of the nonzero Im n_{eff} predicted by the EMG theory. We note that for a laser intensity of 0.01 W/μm^2, the force unit $\epsilon_0 S_t^2 E_0^2 \cong 2.8$ fN. We observe that within the regions where n_{eff} becomes negative, so does the corresponding EM force. Within the first NRI we identify two main dips of the force due to Mie resonances of the sphere. In Fig. 2(e) we show the spectrum of $F/(\epsilon_0 S_t^2 E_0^2)$ when the test sphere is immersed in the middle of a 512-planes-thick metamaterial slab and the slab is illuminated from the left by a normally incident plane wave. Within the NRI regions of Fig. 2(b) we observe that, more or less, the corresponding force assumes negative values. However, within the same NRI region, the force may assume positive values too. This is most apparent in the first NRI region. In order to study this in more detail, in Fig. 3, we show the contribution of different **g** components of Eq. (1) to the total force within the first NRI band. We note that all **g** vectors of the same magnitude, i.e., $2\pi/a_0(\pm,1,0)$, $2\pi/a_0(0,\pm 1)$, and $2\pi/a_0(\pm 1,\pm 1)$, correspond to the same force spectrum. We see that the $\mathbf{g}=\mathbf{0}$ force component remains negative within the whole NRI region while the other **g** components become positive at the low-frequency part of the NRI band resulting in positive total force. The behavior of the $\mathbf{g}=\mathbf{0}$ component is more or less expected as it is the only meaningful component in an effective-medium treatment of the metamaterial which describes it as a homogeneous medium n_{eff}. The other components with $\mathbf{g}\neq\mathbf{0}$ cannot be described by any kind of effective-medium theory since the corresponding wave number q can never reach the $q\rightarrow 0$ limit. This is the same problem pointed out previously concerning the reduced translational symmetry (periodicity) of the metamaterials [14].

In the inset of Fig. 3 we show the contribution to the force of the component $\mathbf{g}=2\pi/a_0(1,1)$, for two different slab thicknesses. We see that both curves are described by the same envelope function and differ only in the density of the Fabry-Pérot peaks. The same picture holds for the other **g** components. This is in accordance with our previous remark on the Bloch nature of the EM field within a metamaterial which suggests that the EM force exerted on a particle results from the gradient of the field intensity rather than from radiation pressure.

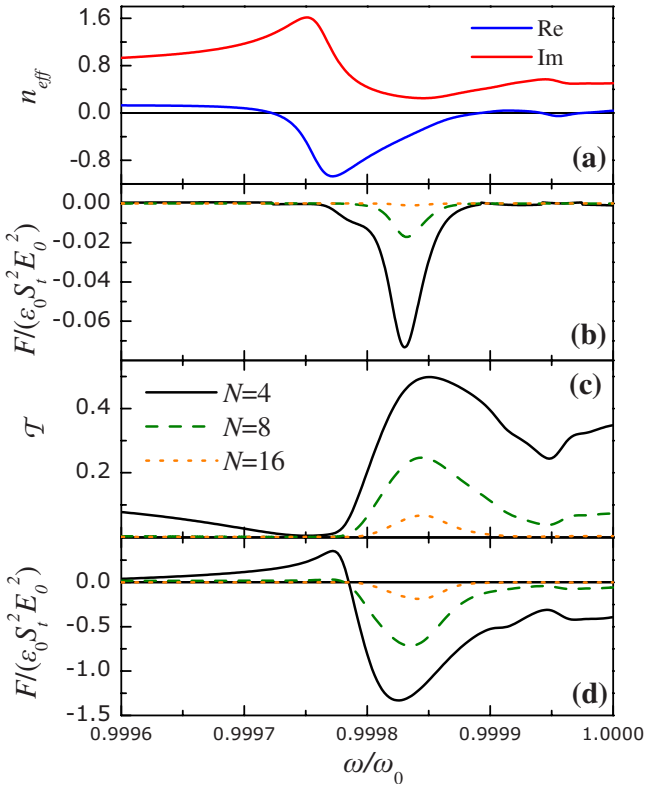

FIG. 4. (Color online) (a) Real and imaginary parts of the effective refractive index n_{eff} of a 3D array of *lossy* close-packed metal-coated CuCl spheres of radius $S=28$ nm and coating thickness $\ell=2.8$ nm, as calculated by the EMG method. (b) Spectrum of the EM force exerted on a polystyrene ($\epsilon=2.56$) nanosphere of radius $S=2.9$ nm embedded in a homogeneous medium described by n_{eff} depicted in (a). The EM wave reaching the test sphere is generated at a distance from the sphere equal to the thickness of $N=4,8,16$ planes of nanospheres. (c) Transmittance curve for light incident normally on slabs consisting of $N=4,8,16$ (001) planes of an fcc crystal of the above nanospheres. (d) Spectrum of the EM force exerted on the same sphere as in (b), embedded in the middle of a metamaterial slab of $N=4,8,16$ planes of spheres. The nanosphere is placed within the slab as in Fig. 2(e).

Next, we restore the actual losses in the constituent materials of the nanospheres ($\hbar\gamma_s=5\times10^{-5}$ eV, $\gamma_m/\omega_p=0.01$). In Figs. 2 and 3 we have placed the test sphere within a very thick slab in order to simulate a bulk sample (EM force practically independent of the number of planes). However, when losses are taken into account, the transmitted EM wave reaching the test sphere in such a thick slab will be severely attenuated resulting in an almost negligible EM force. Therefore, we have considered thinner slabs consisting of $N=4,8,16$ planes of spheres. Figure 4 is the same as Fig. 2 but with absorption taken into account and for thinner slabs. Also, in Fig. 4(b), the distance of the source of the plane

wave from the test sphere is taken equal to the thickness of $N=4,8,16$ planes of spheres, in order to include the effect of wave attenuation within the metamaterial slab. A frequency band structure in Fig. 4 is meaningless as there are no Bloch waves in an infinite, absorbing crystal. By comparing Figs. 2(a) and 4(a) it is evident that the rich structure of Fig. 2(a) is lost apart from a single resonance. This is due to the short lifetime of the resonant states of Fig. 2 compared to the inverse of the material losses (relaxation times). We observe that the force acting on the test sphere as predicted by the EMG theory [Fig. 4(b)] is in good agreement with that obtained by the LMS method (Fig. 4(d)]. Both forces are smaller than those of Fig. 2 due to the attenuation (absorption) experienced by the incident wave on its way to the test sphere in the middle of the metamaterial slab. In the case of the EMG result, the attenuation is higher as it overestimates Im n_{eff} (see above).

The phenomenon of the reversed EM force can be experimentally verified by slowly infiltrating nanoparticles or quantum dots (test particles) in the middle of the slab under continuous illumination, say, from the left surface of the slab. The infiltration process can be similar to the one followed for the creation of inverted photonic structures [15]. For sufficiently strong laser power, the EM force can overcome other forces (gravitational, van der Waals) and in the event of radiation attraction, it will force the infiltrated particles to be deposited on the metal-coated CuCl spheres of the left-half slab (in the case of radiation repulsion the infiltrated particles will be deposited on the right-half slab). The amount of deposition of particles on the left-half slab can be recovered by contemporary microscopy techniques which can probe the interior of a given sample such as the cross-sectional transmission electron microscopy (XTEM) [16] or cross-sectional scanning-tunneling microscopy (STM) [17].

In conclusion, by employing rigorous EM calculations we have verified that in general, within an NRI frequency band, a test particle immersed within a metamaterial slab experiences an EM attraction under illumination. When the material losses are assumed negligible, due to the unavoidable inherent periodicity of a metamaterial, inhomogeneous waves generated from the diffraction of an incident plane wave at the surface of the metamaterial may result in a total EM repulsion within an NRI band, as these waves do not comply with any effective-medium description (EMG theory in our case). When considering a causal metamaterial by taking into account material losses, both effective medium theory and rigorous EM calculations predict an attractive force exerted on a particle under illumination.

We thank Professor P. Poulopoulos for helpful discussions. This work was supported by the "Karatheodory" research fund of University of Patras.

[1] A. Lakhtakia and T. G. Mackay, Opt. Photonics News **18**, 32 (2007).
[2] V. G. Veselago, Sov. Phys. Usp. **10**, 509 (1968).
[3] J. B. Pendry, Phys. Rev. Lett. **85**, 3966 (2000).
[4] R. A. Shelby, D. R. Smith, and S. Schultz, Science **292**, 77 (2001).
[5] A. Grbic and G. V. Eleftheriades, Phys. Rev. Lett. **92**, 117403 (2004).
[6] J. Lu *et al.*, Opt. Express **11**, 723 (2003).
[7] S. Riyopoulos, Opt. Lett. **31**, 2480 (2006).
[8] B. A. Kemp, J. A. Kong, and T. M. Grzegorczyk, Phys. Rev. A **75**, 053810 (2007).
[9] M. Artoni, G. La Rocca, and F. Bassani, Phys. Rev. E **72**, 046604 (2005).
[10] V. Yannopapas and N. V. Vitanov, Phys. Rev. B **74**, 193304 (2006).
[11] M. S. Wheeler, J. S. Aitchison, and M. Mojahedi, Phys. Rev. B **73**, 045105 (2006).
[12] R. Ruppin, Opt. Commun. **182**, 273 (2000).
[13] N. Stefanou, V. Yannopapas and A. Modinos, Comput. Phys. Commun. **113**, 49 (1998); **132**, 189 (2000).
[14] T. Koschny, P. Markos, E. N. Economou, D. R. Smith, D. C. Vier, and C. M. Soukoulis, Phys. Rev. B **71**, 245105 (2005).
[15] A. Blanco *et al.*, Nature (London) **405**, 437 (2000).
[16] C. S. Kim *et al.*, Phys. Rev. Lett. **85**, 1124 (2000).
[17] A. Mikkelsen *et al.*, Nat. Mater. **3**, 519 (2004).